Journal of Structural Geology 30 (2008) 868–875

Contents lists available at ScienceDirect

Journal of Structural Geology

journal homepage: www.elsevier.com/locate/jsg

A graphical–algebraic method for analysing shear zone displacements from observations on arbitrarily oriented outcrop surfaces

Susanne Grigull *, Timothy A. Little [1]

School of Geography, Environment and Earth Sciences, Victoria University of Wellington, PO Box 600, Wellington 6140, New Zealand

ARTICLE INFO

Article history:
Received 18 July 2007
Received in revised form 14 February 2008
Accepted 4 March 2008
Available online 12 March 2008

Keywords:
Shear zones
Finite slip
Fault offsets
Displacement
Movement plane
Matlab

ABSTRACT

We present a practical graphical–algebraic method that enables one to achieve the true displacement and shape of deformed geological markers in fault or shear zones as observed on arbitrarily oriented outcrop surfaces. We use as our natural example deformed quartz veins that have been sheared across brittle–ductile faults in the Southern Alps of New Zealand. The technique is based on the assumption that simple shear has dominated the shear zone formation. For input data we require the strikes and dips of the outcrop surfaces, the offset markers, and the shear zones as well as the pitch of the simple shear vector in the plane of the shear zone. The paper develops a set of algebraic and graphical operations that allow one to convert photographs of faulted or sheared planar markers observed on an arbitrary outcrop surface into an equivalent view that is coincident with the movement (m) plane of the fault or shear zone. This view displays the true displacement of the offset marker and delineates its deformed shape as seen in a section that is parallel to the slip vector.

1. Introduction

When investigating planar geological structures in the field that show an offset of older marker planes (e.g. fault zones and shear zones) we have to deal with the fact that in many cases the outcrop plane does not coincide with the movement plane (i.e. the plane perpendicular to the fault or shear zones, that coincides with the true slip direction). This is crucial, for example, if maps or photographs are used to constrain the rheology of rocks (e.g. Talbot, 1999; Pennacchioni, 2005; Fusseis et al., 2006). Ignoring the "distorted" nature of fault or shear zone offset geometries on arbitrary outcrop planes can yield inaccurate measurements of slip or shear strain, and of the deformed shape of offset markers.

This paper offers a "recipe" on how to translate geological offset data from an arbitrary outcrop plane onto the movement plane.[2] The paper is based on geological investigations of rocks in a fault array that has been exhumed from mid-lower crustal depths (~20 km) and is now exposed in glaciated outcrops in the central Southern Alps, New Zealand. Here, faults brittlely offset biotite-zone Alpine Schist, and – where the tips of these faults encounter older quartz veins that are hosted by these schists – they terminate into local ductile shear zones in the quartz veins (Fig. 1).

As a first step towards retrieving rheological information from the deformed shape of the marker veins, the exposures were photographed and measurements were made of the fault attitudes (strike and dip), the quartz marker vein attitudes (strike and dip), the pitch of the slip lineations in the fault planes, and the strikes and dips of the outcrop surfaces. Unfortunately, rarely do the glaciated outcrop surfaces coincide exactly with the actual movement plane. Digitising the photographs of the faults and the quartz veins' offset across them enabled us to extract x–y coordinates for the fault and vein margins in the outcrop plane. We then projected these x–y data onto the movement plane to derive a depiction of the true offsets and shapes of the displaced planar markers.

2. Assumptions

Before projecting the data onto the movement plane, several assumptions must be made:

(1) that the fault plane orientation, the marker vein orientation, the trend and plunge of the slip lineation on the fault surface, and the outcrop orientation are accurately known;
(2) that the observed slip lineation is a faithful indicator of the finite slip direction, and that it is viewable nearby on some other outcrop plane, or is otherwise known;

* Corresponding author. Tel.: +64 4 463 5233x8375; fax: +64 4 463 5186.
E-mail addresses: susanne.grigull@vuw.ac.nz (S. Grigull), tim.little@vuw.ac.nz (T.A. Little).
[1] Tel.: +64 4 463 6198; fax: +64 4 463 5186.
[2] Interested researchers can contact the corresponding author for an electronic copy of a Matlab7 script (including a short manual on using the script) that can read and process their data as described in the paper and outputs the data in a plot similar to Fig. 5c.

0191-8141/$ – see front matter © 2008 Elsevier Ltd. All rights reserved.
doi:10.1016/j.jsg.2008.03.001

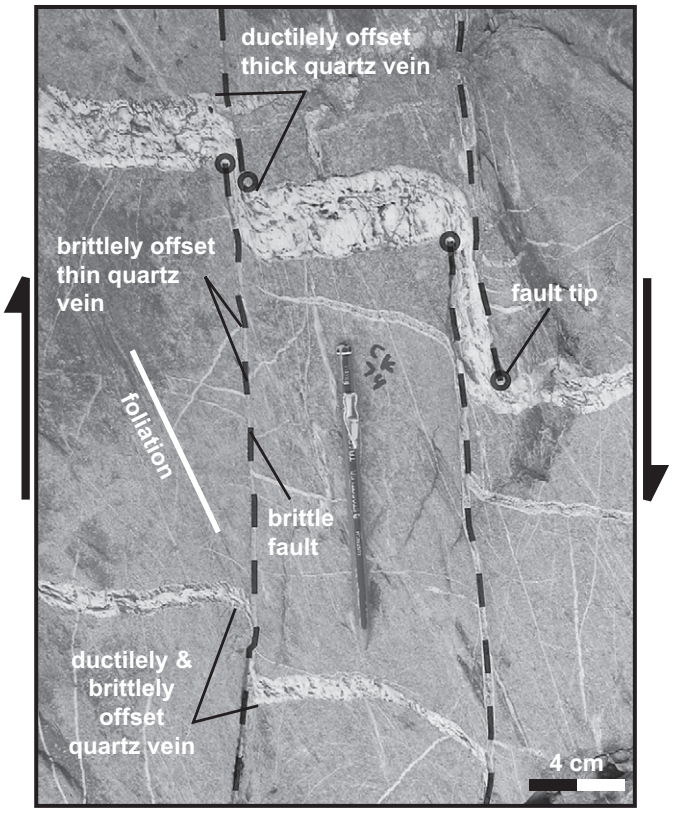

Fig. 1. Outcrop photograph showing brittle faults (stippled lines) terminating into quartz veins and offsetting them ductilely to brittlely. Location: Crawford Knob, central Southern Alps, New Zealand.

(3) that the fault plane can be approximated to be a flat, non-bending surface;
(4) that the orientation and thickness of the original marker vein did not, prior to offset, change in the third dimension, i.e. that it was laterally continuous and tabular in shape;
(5) that the subsequent deformational curvature of this marker was the result of simple shear, thus leading to a cylindrical "drag fold" geometry for the now deformed marker (Ramsay and Huber, 1987, p. 509);
(6) that photographs have been taken normal to the outcrop surface, or that it is possible to undistort photographs that were taken at an oblique angle using, e.g. the method of Cooper and Bamford (1987), or alternatively, that tracings have been taken directly from the outcrop.

3. Preparing *x–y–z* data from photographs (Step 1)

For the denotation of vectors, variables and coefficients refer to the glossary in Appendix A.

3.1. Coordinate systems

In this paper, the right-hand-rule applies for all geological orientation measurements, where the thumb represents the strike of a plane and the index finger points into the dip direction. All planar measurements are given in 'strike/dip' and all linear measurements in 'trend/plunge'.

All Cartesian coordinate systems used in this paper are right-handed. A geographical and an outcrop coordinate system have been defined that have a common spatial origin located on the fault trace in the outcrop plane at the midpoint of the two halves of an offset marker vein (star in Fig. 2). The *geographical coordinate system* has got the axes x_g = North, y_g = East, and z_g = "down", where $\hat{\vec{x}}_g = \begin{pmatrix}1\\0\\0\end{pmatrix}$, $\hat{\vec{y}}_g = \begin{pmatrix}0\\1\\0\end{pmatrix}$, and $\hat{\vec{z}}_g = \begin{pmatrix}0\\0\\1\end{pmatrix}$ are the unit vectors that point along the respective axes. The *outcrop coordinate system* is spanned by the axes x_{oc}, y_{oc}, and z_{oc}, where the positive x_{oc}-axis is equivalent to the fault trace on the outcrop and pointing in the down-plunge direction of that trace. y_{oc} lies in the outcrop face pointing 90° clockwise from the fault trace with respect to the positive z_{oc}-axis. z_{oc} is represented by the pole to the outcrop surface pointing "inwards" (Fig. 2). $\hat{\vec{x}}_{oc} = \begin{pmatrix}x_g^{x_{oc}}\\y_g^{x_{oc}}\\z_g^{x_{oc}}\end{pmatrix}$, $\hat{\vec{y}}_{oc} = \begin{pmatrix}x_g^{y_{oc}}\\y_g^{y_{oc}}\\z_g^{y_{oc}}\end{pmatrix}$ and $\hat{\vec{z}}_{oc} = \begin{pmatrix}x_g^{z_{oc}}\\y_g^{z_{oc}}\\z_g^{z_{oc}}\end{pmatrix}$ are the unit vectors of the outcrop coordinate system, cast in terms of their geographical coordinates.

In order to determine $\hat{\vec{x}}_{oc}$, we first need to find the orientation of the pole to the outcrop plane and the pole to the fault plane in the geographical coordinate system by calculating the *direction cosines* (Appendix B.1) of those poles from the strike and dip angles of the respective planes. The pole to the outcrop plane yields $\hat{\vec{z}}_{oc}$. The pole to the fault plane yields the unit vector $\hat{\vec{f}}$ (Fig. 3a). The normalised right-handed cross-product of $\hat{\vec{z}}_{oc} \times \hat{\vec{f}}$ results in $\hat{\vec{x}}_{oc}$, the unit vector parallel to the fault trace on the outcrop surface. To ensure consistency for the following transformations, we define $\hat{\vec{x}}_{oc}$ to always point downwards along the outcrop surface, i.e. if $\hat{\vec{z}}_{oc} \times \hat{\vec{f}}$ results in a negative value for $z_g^{x_{oc}}$, we have to multiply the coordinates for $\hat{\vec{x}}_{oc}$ by (−1). The normalised right-handed cross-product $\hat{\vec{z}}_{oc} \times \hat{\vec{x}}_{oc}$ will then result in the Cartesian vector coordinates for $\hat{\vec{y}}_{oc}$ (Fig. 2).

3.2. Digitising

For the projection of the marker veins onto the movement plane, they need to be digitised. In a graphics programme (e.g. Adobe Illustrator) the photograph is rotated in such a way that the positive x_{oc}-axis (i.e. down-plunge "end" of the fault trace) points towards the top. The positive y_{oc}-axis should now point to the right. The rotated photograph is then resized to a desired scale, imported into a digitising programme (e.g. Replica by Graphic Edge Ltd.) and digitised. For this, the origin is chosen such that it lies on the midpoint between the two offset parts of the markers. This origin corresponds to the spatial origin (star) in Fig. 2 and will remain the same throughout the following coordinate transformations. The digitising outputs are coordinates of points in the x_{oc}–y_{oc} plane of the outcrop coordinate system, with $z_{oc} = 0$. Note that most digitising softwares use left-handed coordinate systems, and close attention has to be paid not to confuse the *x*- and *y*-coordinates.

3.3. Geographical coordinates of points

Now the position of the digitised points has to be recast in terms of the geographical coordinate system. As the outcrop and geographical coordinate systems both have the same origin, a *change of orthonormal basis* can be performed using Eqs. (1a) and (1b), below, in order to transform the outcrop coordinates of a point P $(x_{oc}^P, y_{oc}^P, z_{oc}^P = 0)$ into its geographical coordinates $P\,(x_g^P, y_g^P, z_g^P)$.

$$P{:=}\overrightarrow{p} = \begin{pmatrix} x_g^P \\ y_g^P \\ z_g^P \end{pmatrix} = \begin{bmatrix} \widehat{\overrightarrow{x}}_g \cdot \widehat{\overrightarrow{x}}_{oc} & \widehat{\overrightarrow{x}}_g \cdot \widehat{\overrightarrow{y}}_{oc} & \widehat{\overrightarrow{x}}_g \cdot \widehat{\overrightarrow{z}}_{oc} \\ \widehat{\overrightarrow{y}}_g \cdot \widehat{\overrightarrow{x}}_{oc} & \widehat{\overrightarrow{y}}_g \cdot \widehat{\overrightarrow{y}}_{oc} & \widehat{\overrightarrow{y}}_g \cdot \widehat{\overrightarrow{z}}_{oc} \\ \widehat{\overrightarrow{z}}_g \cdot \widehat{\overrightarrow{x}}_{oc} & \widehat{\overrightarrow{z}}_g \cdot \widehat{\overrightarrow{y}}_{oc} & \widehat{\overrightarrow{z}}_g \cdot \widehat{\overrightarrow{z}}_{oc} \end{bmatrix} \cdot \begin{pmatrix} x_{oc}^P \\ y_{oc}^P \\ z_{oc}^P \end{pmatrix}, \quad (1a)$$

where $P{:=}\overrightarrow{p}$ means that the coordinates of point P are defined by its position vector $\overrightarrow{p}$ that is anchored at the common spatial origin (0, 0, 0).

Knowing that $\widehat{\overrightarrow{x}}_g = \begin{pmatrix} 1 \\ 0 \\ 0 \end{pmatrix}$, $\widehat{\overrightarrow{y}}_g = \begin{pmatrix} 0 \\ 1 \\ 0 \end{pmatrix}$, and $\widehat{\overrightarrow{z}}_g = \begin{pmatrix} 0 \\ 0 \\ 1 \end{pmatrix}$, Eq. (1a) can be simplified to

$$P{:=}\overrightarrow{p} = \begin{pmatrix} x_g^P \\ y_g^P \\ z_g^P \end{pmatrix} = \begin{bmatrix} x_g^{x_{oc}} & x_g^{y_{oc}} & x_g^{z_{oc}} \\ y_g^{x_{oc}} & y_g^{y_{oc}} & y_g^{z_{oc}} \\ z_g^{x_{oc}} & z_g^{y_{oc}} & z_g^{z_{oc}} \end{bmatrix} \cdot \begin{pmatrix} x_{oc}^P \\ y_{oc}^P \\ z_{oc}^P \end{pmatrix}. \quad (1b)$$

This operation results in the vector components of vector $\overrightarrow{p}$ determining the position of a digitised point P in the geographical reference system.

4. Projection into the movement plane (Step 2)

4.1. The movement plane (m-plane) in point-normal form

The movement plane or "m-plane" (Fig. 3a) is perpendicular to the fault plane and parallel to the unit vector of the direction of movement (i.e. parallel to the slip lineation). The pole to the m-plane $\widehat{\overrightarrow{m}}$ in geographical coordinates can therefore be calculated from the right-handed cross-product of the unit vector $\widehat{\overrightarrow{s}}$ parallel to the slip direction and the unit vector $\widehat{\overrightarrow{f}}$ parallel to the pole of the fault plane:

$$\widehat{\overrightarrow{m}} = \frac{\widehat{\overrightarrow{s}} \times \widehat{\overrightarrow{f}}}{|\widehat{\overrightarrow{s}} \times \widehat{\overrightarrow{f}}|} = \begin{pmatrix} x_m \\ y_m \\ z_m \end{pmatrix} \quad (2)$$

$\widehat{\overrightarrow{m}}$ originates at the spatial origin of all coordinate systems.

In algebraic terms a plane in 3-space is uniquely defined by a point that lies within the plane and a vector normal to the plane, so that the point-normal form of the equation of the movement plane M becomes

$$M{:=}\overrightarrow{r} \cdot \widehat{\overrightarrow{m}} = 0 \quad (3)$$

where $\overrightarrow{r}$ is a vector in the m-plane.

4.2. The projection vector and projection line

Similar to the axes of drag folds (Ramsay and Huber, 1987, their Fig. 23.9) the projection vector $\widehat{\overrightarrow{v}}$ corresponds to the intersection lineation of the fault surface and the marker vein (Fig. 3b). $\widehat{\overrightarrow{v}}$ is independent of the direction of movement and only depends on the marker vein orientation and the orientation of the fault plane. In fact, $\widehat{\overrightarrow{v}}$ is parallel to both. Thus, the projection vector $\widehat{\overrightarrow{v}}$ is given by the cross-product of the pole to the fault surface $\widehat{\overrightarrow{f}}$ and the pole to the marker vein $\widehat{\overrightarrow{q}}$:

$$\widehat{\overrightarrow{v}} = \frac{\widehat{\overrightarrow{f}} \times \widehat{\overrightarrow{q}}}{|\widehat{\overrightarrow{f}} \times \widehat{\overrightarrow{q}}|} = \begin{pmatrix} x_v \\ y_v \\ z_v \end{pmatrix} \quad (4)$$

In Eq. (4) the order of terms in the cross-product does not matter as the projection vector is only used as a direction vector for the 'projection line'.

The projection line (Fig. 3a) runs through the point $P(x_g^P, y_g^P, z_g^P)$ sitting on the outcrop surface and is parallel to the projection vector. The point P' $(x_g^{P'}, y_g^{P'}, z_g^{P'})$ at which the projection line cuts through the m-plane is the projection of point P onto the movement plane.

A line in 3-space is determined uniquely by specifying a point on the line and a non-zero vector parallel to the line so that the vector equation of the projection line l becomes

$$l{:=}\overrightarrow{r} = \overrightarrow{p} + \lambda\widehat{\overrightarrow{v}} \quad (5)$$

where $\overrightarrow{r}$ is a vector that is anchored at the spatial origin and pointing to any point on the projection line l and $\overrightarrow{p} = \begin{pmatrix} x_g^P \\ y_g^P \\ z_g^P \end{pmatrix}$ is the position vector of point P in the geographical coordinate system derived from Eq. (1b), $\widehat{\overrightarrow{v}}$ is the projection vector derived from Eq. (4), and λ is a scalar parameter with $-\infty < \lambda < +\infty$ which reflects the fact that the line extends indefinitely.

4.3. The projection process

In order to find the point P', where the projection line cuts the m-plane, Eqs. (2) and (5) need to be inserted into Eq. (3) and the resulting equation be solved for λ:

$$\lambda = -\frac{x_m x_g^P + y_m y_g^P + z_m z_g^P}{x_m x_v + y_m y_v + z_m z_v} \quad (6)$$

Placing λ back into Eq. (5) and solving for all vector coordinates leads to the coordinates of P':

$$P'{:=}\overrightarrow{r} = \begin{pmatrix} x_g^P \\ y_g^P \\ z_g^P \end{pmatrix} - \frac{x_m x_g^P + y_m y_g^P + z_m z_g^P}{x_m x_v + y_m y_v + z_m z_v} \begin{pmatrix} x_v \\ y_v \\ z_v \end{pmatrix} = \begin{pmatrix} x_g^{P'} \\ y_g^{P'} \\ z_g^{P'} \end{pmatrix} \quad (7)$$

5. Plan view of the *m*-plane (Step 3)

In order to achieve a plan view of the projected marker points on the m-plane, the strike and dip of the m-plane ($\text{strike}_{\text{m-plane}}$, $\text{dip}_{\text{m-plane}}$, Appendix B.2) needs to be found and a rotation in 3-space undertaken, to bring that plane and its points into horizontality and to a position where all fault traces on the m-plane are parallel to one another. This rotation is divided into three subrotations (Eqs. (8a), (8b), and (11)). The strike line of the m-plane is the rotation axis for the first two subrotations. First, the points on the m-plane are rotated about the vertical axis (z_g) until the strike line of the m-plane is E–W, i.e. parallel to y_g. After this first rotation, the m-plane dips towards the negative x_g-direction. This rotation is called "rot1", and the new position vectors of the projected points are called $\overrightarrow{p}'_{\text{rot1}}$:

$$P'_{\text{rot1}}{:=}\overrightarrow{p}'_{\text{rot1}} = \begin{pmatrix} x_{\text{rot1}}^{P'} \\ y_{\text{rot1}}^{P'} \\ z_{\text{rot1}}^{P'} \end{pmatrix} = \begin{pmatrix} x_g^{P'} \cos\psi - y_g^{P'} \sin\psi \\ x_g^{P'} \sin\psi + y_g^{P'} \cos\psi \\ z_g^{P'} \end{pmatrix} \quad (8a)$$

The rotation angle for this first step is $\psi = 90^\circ - \text{strike}_{\text{m-plane}}$. For those strike angles between 0° and 90°, ψ will be positive and the rotation will be anticlockwise with respect to the positive z_g-axis. For all other orientations, ψ will be negative and the rotation clockwise. Eq. (8a) rotates point P' (Eq. (7)) about the z_g-axis and results in point P'_{rot1}.

In the second step the coordinates of point P'_{rot1} derived from Eq. (8a) are rotated about the now strike-parallel, E–W y_g-axis

(Eq. (8b)). This rotation is called "rot2". As point P'_{rot1} is part of the dipping m-plane, the rotation angle for the rotation about the y_g-axis becomes $\varphi = -\mathrm{dip}_{m\text{-plane}}$ and the rotation is clockwise with respect to the positive y_g-axis.

$$P'_{rot2} := \overrightarrow{p}'_{rot2} = \begin{pmatrix} x^{P'}_{rot2} \\ y^{P'}_{rot2} \\ z^{P'}_{rot2} \end{pmatrix} = \begin{pmatrix} x^{P'}_{rot1}\cos\varphi + z^{P'}_{rot1}\sin\varphi \\ y^{P'}_{rot1} \\ -x^{P'}_{rot1}\sin\varphi + z^{P'}_{rot1}\cos\varphi \end{pmatrix} \tag{8b}$$

Eqs. (8a) and (8b) can be merged into Eq. (8c), where P'_{rot12} is the projection of point P onto the movement plane and in plan view of the movement plane. The $z^{P'}_{rot12}$-coordinate of point P'_{rot12} must be 0 after the rotation.

$$\begin{aligned} P'_{rot12} := \overrightarrow{p}'_{rot12} &= \begin{pmatrix} x^{P'}_{rot12} \\ y^{P'}_{rot12} \\ z^{P'}_{rot12} \end{pmatrix} \\ &= \begin{pmatrix} \left(x^{P'}_{g}\cos\psi - y^{P'}_{g}\sin\psi\right)\cos\varphi + z^{P'}_{g}\sin\varphi \\ x^{P'}_{g}\sin\psi + y^{P'}_{g}\cos\psi \\ -\left(x^{P'}_{g}\cos\psi - y^{P'}_{g}\sin\psi\right)\sin\varphi + z^{P'}_{g}\cos\varphi \end{pmatrix} \end{aligned} \tag{8c}$$

After having rotated the m-plane and its points into horizontality, the trace line of the fault on the m-plane need not necessarily be exactly N–S (i.e. up and down the page). The second step of this rotation in 3-space aims to make the plots of the shapes and offsets of multiple cases of displaced markers easily comparable, i.e. we need to rotate all projected points lying in the m-plane to a position where the fault traces of all cases are parallel to one another. The easiest solution to this problem is to conduct one further rotation ("rot3") of each point about the vertical z_g-axis (this is the pole to the now horizontal m-plane). This final rotation will align all the fault traces in the m-plane into N–S parallelism through the spatial origin. The trace $\overrightarrow{t}$ of a fault on the m-plane is the intersection between the fault plane and the m-plane. $\overrightarrow{t}$ is therefore the right-handed normalised cross-product of the pole to the m-plane $\overrightarrow{m}$ and the pole to the fault $\overrightarrow{f}$:

$$\overrightarrow{t} = \frac{\overrightarrow{m} \times \overrightarrow{f}}{|\overrightarrow{m} \times \overrightarrow{f}|} = \begin{pmatrix} x_t \\ y_t \\ z_t \end{pmatrix} \tag{9}$$

We define $\overrightarrow{t}$ to always point downwards, i.e. if z_t is negative, we additionally need to multiply Eq. (9) by the factor (-1).

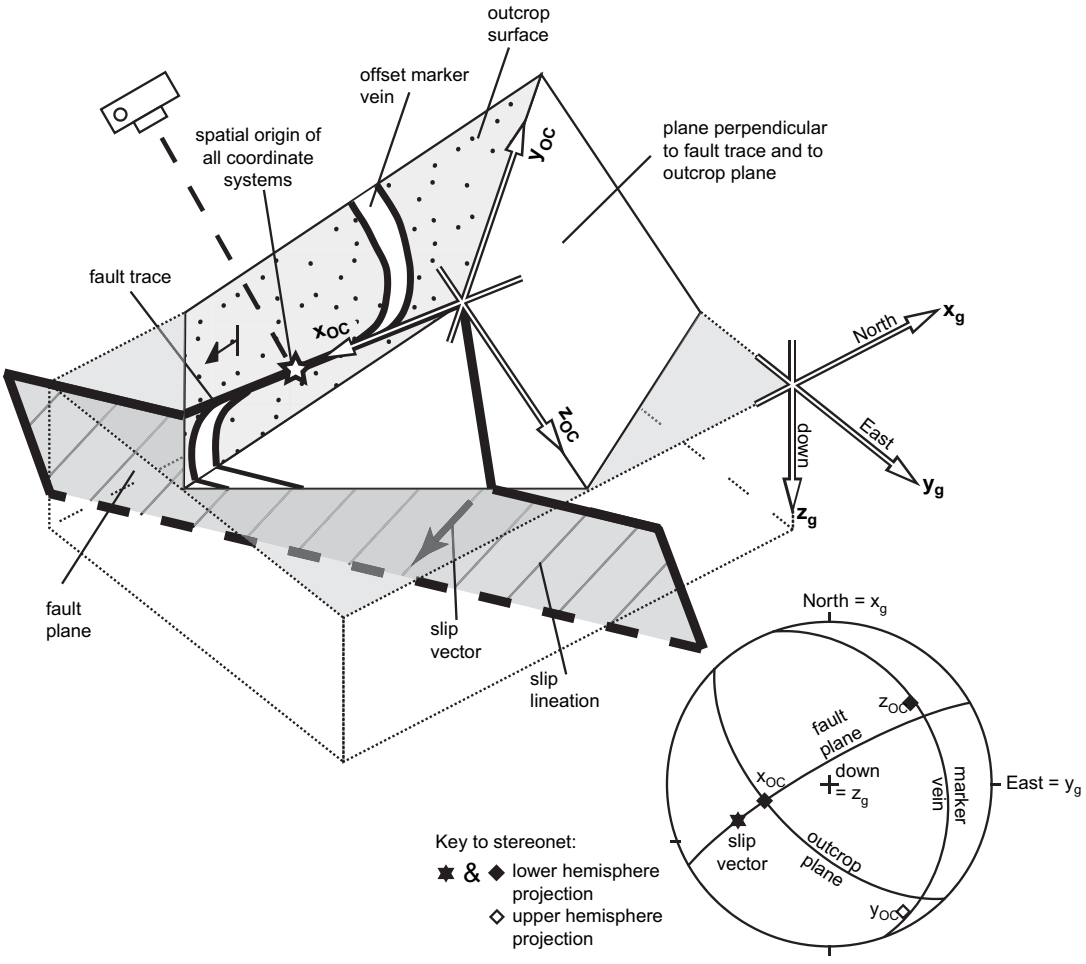

Fig. 2. Bock diagram illustrating the spatial relationship between the outcrop plane and the fault plane as well as the two coordinate systems defined in Appendix 3.1 (x_{oc}: x-axis of the outcrop coordinate system, parallel and down-plunge to the fault trace and lying within the outcrop plane; y_{oc}: at a right angle to x_{oc} and lying within the outcrop surface; z_{oc}: pole to the outcrop plane; x_g, y_g, z_g: geographical coordinate axes). The spatial origin common to both coordinate systems is indicated by the white star. Due to clarity, the axes of the outcrop and geographical coordinate systems have been shifted away from the origin. In an ideally taken photograph, the photo axis (stippled line between camera and outcrop) is perpendicular to the outcrop surface (cf. assumption (6) in 2.). The corresponding planes, the slip vector and the three axes of the outcrop coordinate system are plotted in a lower hemisphere stereonet. Note that y_{oc} is pointing upwards in the block diagram and would therefore plot on the upper hemisphere. The stereonet displays the negative end of the y_{oc}-axis.

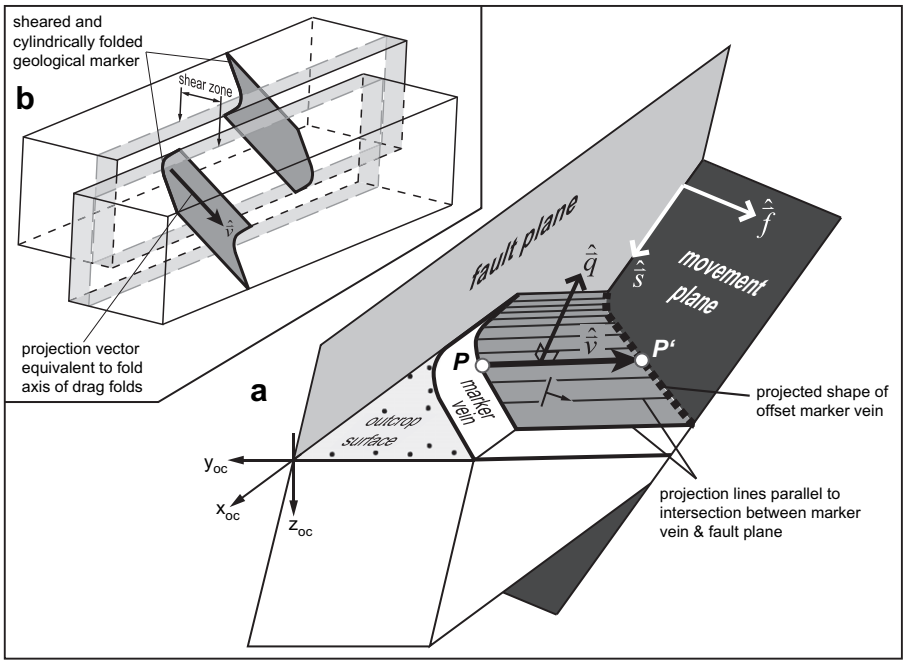

Fig. 3. (a) Block diagram showing the downthrown half of a shear zone and the relationships between fault plane and movement plane as well as fault plane, marker vein and projection vector. $\hat{\boldsymbol{s}}$ (slip vector) and $\hat{\boldsymbol{f}}$ (pole to fault plane) span the movement plane. The cross-product of $\hat{\boldsymbol{q}}$ (pole to marker vein) and $\hat{\boldsymbol{f}}$ results in the projection vector $\hat{\boldsymbol{v}}$. Point P' is the projection of point P onto the movement plane along a projection line parallel to $\hat{\boldsymbol{v}}$. The stippled bold black line represents the projected shape of the marker vein on the m-plane. (b) Block diagram showing the concept for deriving the projection vector $\hat{\boldsymbol{v}}$. Assuming that the deformation of the geological marker (dark grey) was due to simple shear, $\hat{\boldsymbol{v}}$ is equivalent to the fold axis of the geological marker, and corresponds to the intersection of the geological marker and the shear plane. The area shaded in light grey indicates the extent of the shear zone and the stippled grey lines mark the shear zone boundaries.

Applying the rotation in Eq. (8c) to $\hat{\overline{t}}$ yields horizontality of the fault trace in the m-plane. We call the resulting vector $\hat{\overline{t}}'_{\mathrm{rot12}} = \begin{pmatrix} x^{t'}_{\mathrm{rot12}} \\ y^{t'}_{\mathrm{rot12}} \\ z^{t'}_{\mathrm{rot12}} \end{pmatrix}$.

The rotation angle for this third rotation ("rot3") is the angle δ (Fig. 4) between the positive x_g-axis (North) and the trace of the fault on the horizontal m-plane $\hat{\overline{t}}'_{\mathrm{rot12}}$, that was derived by executing first Eq. (9) and then Eq. (8c). The angle δ is the result of the dot product between $\hat{\overline{x}}_{\mathrm{g}}$ and $\hat{\overline{t}}'_{\mathrm{rot12}}$:

$$\delta = \arccos\left(\hat{\overline{x}}_{\mathrm{g}} \cdot \hat{\overline{t}}'_{\mathrm{rot12}}\right) \tag{10}$$

However, we must take into account that Eq. (10) will only result in values for δ ranging from 0° to 180°. Thus, if $y^{t'}_{\mathrm{rot12}}$ is positive, δ must be negative and the rotation would be clockwise with respect to the positive z_g-axis. If $y^{t'}_{\mathrm{rot12}}$ is negative, we must choose δ to be positive for an anticlockwise rotation about the z_g-axis. The final rotation "rot3" to be applied to all points is then given by the matrix:

$$P'_{\mathrm{rot3}} := \hat{\overline{p}}'_{\mathrm{rot3}} = \begin{pmatrix} x^{P'}_{\mathrm{rot3}} \\ y^{P'}_{\mathrm{rot3}} \\ z^{P'}_{\mathrm{rot3}} \end{pmatrix} = \begin{pmatrix} x^{P'}_{\mathrm{rot12}}\cos\delta - y^{P'}_{\mathrm{rot12}}\sin\delta \\ x^{P'}_{\mathrm{rot12}}\sin\delta + y^{P'}_{\mathrm{rot12}}\cos\delta \\ z^{P'}_{\mathrm{rot12}} \end{pmatrix} \tag{11}$$

6. Examples

In order to demonstrate the usefulness and significance of the projection of geological field data into the movement plane, we chose two examples (Fig. 5) from an exhumed brittle–ductile fault array in the central Southern Alps, New Zealand (e.g. Wightman et al., 2006). The first example is a case, where the orientation of the outcrop plane is not very different from the orientation of the m-plane, whereas in the second example the outcrop orientation differs strongly from the m-plane orientation.

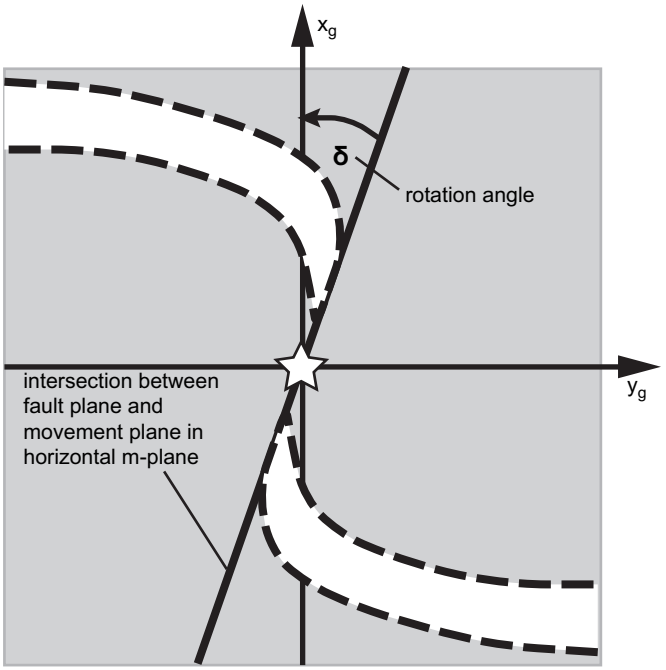

Fig. 4. Schematic diagram of plan view of the movement plane (grey shaded) after the first two rotations "rot1" (Eq. (8a)) and "rot2" (Eq. (8b)). The rotation angle δ for the third rotation "rot3" (Eq. (11)) is the angle between the positive x_g-axis (North) and the trace of the fault plane in the horizontal movement plane.

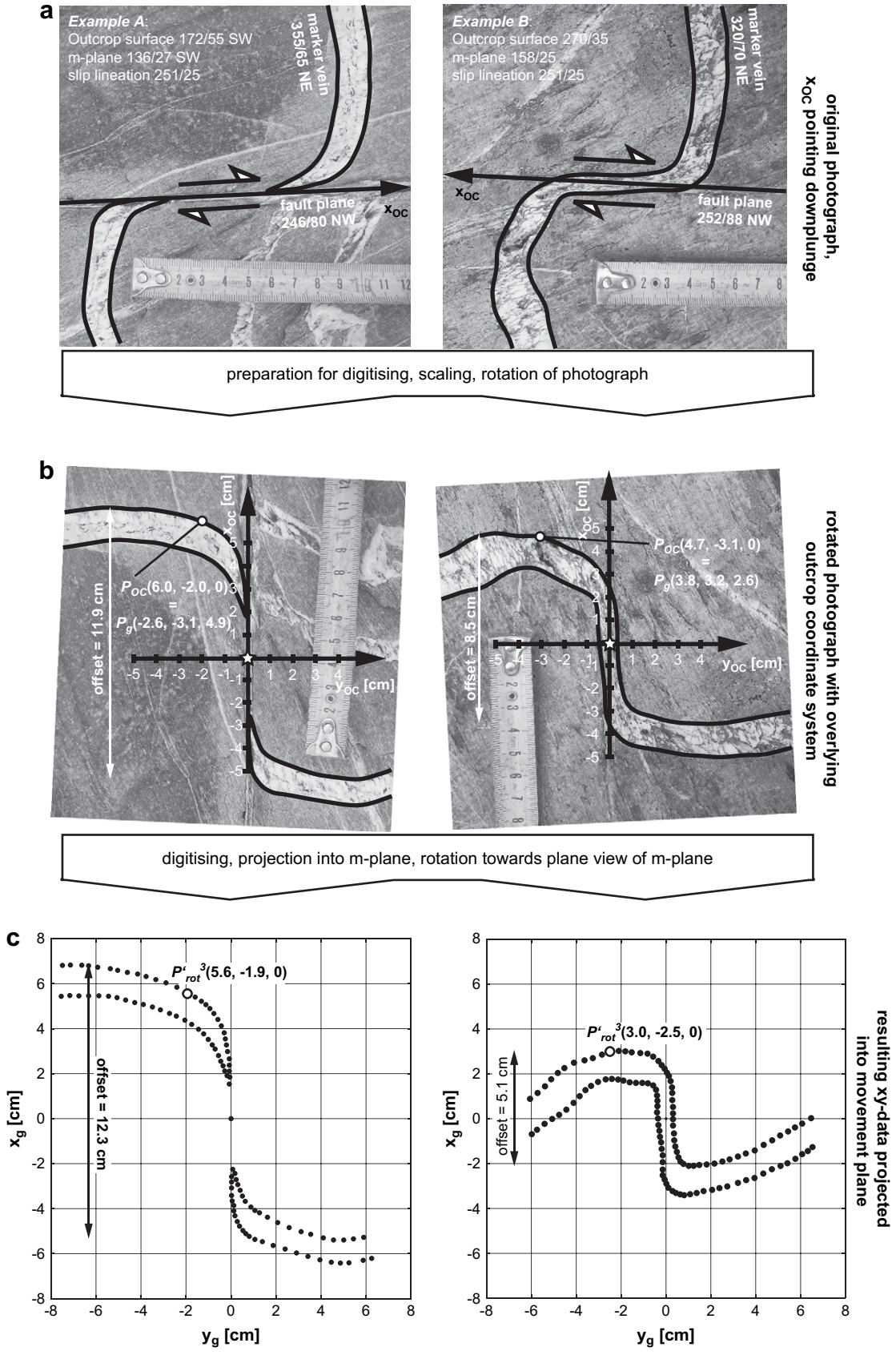

Fig. 5. Flow diagram of the two examples described in the main text. (a) Original photographs with required orientation measurements of planes and slip lineation. (b) Photograph has been rotated such that the x_{oc}-axis points towards the top of the page. The spatial origin of all coordinate systems is marked with a white star. The white circle marks an exemplary digitised point on the boundary between marker vein and wall rock. The point is given in both the coordinates of the outcrop coordinate system and the geographical coordinate system. The white double arrows mark the offsets that were measured on the outcrop surface. (c) The *xy*-data of the marker veins after the projection plotted within the *m*-plane and rotated after Eq. (11). The true offsets within the *m*-plane are marked by black double arrows. The points P'_{rot3} are the projections of the points P_{oc} chosen in (b).

6.1. Example A

The fault in example A strikes at an angle of 246° and dips with 80° towards the NW, the orientation of the marker vein is 355/65 NE and the slip lineation trends 251° and plunges 25°. The outcrop orientation (172/55 SW) differs by 36° in strike angle and by 28° in dip angle from that of the movement plane (136/27 SW). Plotting the transformed coordinates of example A (Fig. 5c) and comparing them to the original coordinates derived from digitising the marker vein on the photograph (Fig. 5b) shows that there is hardly any difference in offset and shape between the original vein and its projection. The curvature of the projected vein is only slightly less, and with 12.3 cm the total offset of the projected vein is only 0.4 cm higher than the one measured in the outcrop plane (11.9 cm).

6.2. Example B

In Example B, the orientation of the fault is 252/88 NW, the marker vein strikes with an angle of 320° and dips 70° to the NE, and the trend and plunge of the slip lineation are the same as in example A (251/25). The difference in strike between the outcrop plane (270/35 N) and the *m*-plane (158/25 SW) is 112° and the difference in dip angles is 10°. The plots in Fig. 5c show that the curvature of the projected vein is significantly higher than the one of the original vein. The total offset of the marker vein measured on the outcrop surface is 8.5 cm, whereas the true offset measured in the movement plane is only 5.1 cm, meaning that the true offset is 3.4 cm (40%) less than the apparent offset measured directly on the outcrop surface.

7. Discussion and conclusions

In this paper we presented a simple method for the translation of geological field data from an outcrop surface into the movement plane of a fault or shear zone. This enables us to calculate true displacements from separation data on outcrop faces and the "true" shape of curved and deformed geological markers. This method is also an algebraic–graphical way to solve for slip from offsets on arbitrary outcrops. If the method described in this paper is used, it is no longer necessary to search for optimally oriented outcrops as, by following the steps above, any outcrop data can be projected into the desired plane, if all variables that are necessary for the projection are known.

As indicated by the two given examples, the projection into the movement plane is especially important for outcrop orientations that deviate strongly from the orientation of the movement plane. However, this is a statement without mathematical proof, and one should consider using the described method for any case of outcrop orientation in order to achieve a high accuracy when investigating offsets and shapes of displaced geological markers. The results of these coordinate transformations clearly depend on the accuracy of the orientation measurements of planes and lineations and also on the verticality of the photo axis with respect to the outcrop surface. Also, if one of the assumptions in 2 is incorrect (e.g. if the deformation was not only due to simple shear) this technique will fail. However, an error propagation analysis would go beyond the scope of this paper and will be left to keen mathematicians.

Acknowledgements

We wish to thank Susan M. Ellis (GNS Science) for constructive and helpful discussions as well as for proof reading this paper. We would also like to thank Declan DePaor and Kieran Mulchrone for thoughtful reviews and comments that significantly improved the original manuscript.

Appendix A. Glossary

A.1. Denotation

$\vec{a}$	Vector a
$\hat{\vec{a}}$	Unit vector in direction of a
$\begin{pmatrix} x_a \\ y_a \\ z_a \end{pmatrix}$	Vector components or coordinates of a
$\vec{a} \times \vec{b}$	Right-handed cross-product
$\vec{a} \cdot \vec{b}$	Dot product
$\lvert\vec{a}\rvert$	Length/norm of a

A.2. Subscripts and superscripts

g	Geographical
oc	Outcrop
m	Movement plane
v	Projection vector
rot	Rotation

A.3. Key

x_g, y_g, z_g	Axes spanning geographical coordinate system
x_{oc}, y_{oc}, z_{oc}	Axes spanning outcrop coordinate system
$\vec{f}$	Vector in direction of pole to fault plane
$\vec{s}$	Slip vector
$\vec{m}$	Vector in direction of pole to m-plane
M	movement plane
$\vec{r}$	Position vector of point P'
$\vec{q}$	Vector in direction of pole to marker vein
$\vec{v}$	Projection vector
I	projection line
λ	Scalar parameter
ψ	Rotation angle for first rotation about z_g-axis
φ	Rotation angle for rotation about y_g-axis
δ	Rotation angle for second rotation about z_g-axis

Appendix B. Conversions

B.1. Conversion from geological attitudes to Cartesian coordinates

Converting the geological attitudes of a plane or a line into Cartesian coordinates means determining *direction cosines* from strike and dip or trend and plunge measurements. Direction cosines are the cosines of the angles α, β, and γ that a vector makes with the positive x, y, and z-axes, respectively. For planes, the direction cosines are calculated after Eq. (B.1-1) and result in a unit normal vector pointing in the direction of the pole to the plane:

$$\hat{\vec{n}}_p = \begin{pmatrix} n_{px} \\ n_{py} \\ n_{pz} \end{pmatrix} = \begin{pmatrix} \cos\alpha \\ \cos\beta \\ \cos\gamma \end{pmatrix} = \begin{pmatrix} \sin\omega\sin\theta \\ -\cos\omega\sin\theta \\ \cos\theta \end{pmatrix}, \tag{B.1-1}$$

where $\hat{\vec{n}}_p$ denotes the unit normal vector of the plane, ω is the strike angle of the plane and θ is the dip angle.

The direction cosines of lines are calculated as in Eq. (B.1-2).

$$\hat{\vec{n}}_l = \begin{pmatrix} n_{lx} \\ n_{ly} \\ n_{lz} \end{pmatrix} = \begin{pmatrix} \cos\alpha \\ \cos\beta \\ \cos\gamma \end{pmatrix} = \begin{pmatrix} \cos\eta\cos\varepsilon \\ \sin\eta\cos\varepsilon \\ \sin\varepsilon \end{pmatrix}, \tag{B.1-2}$$

where $\hat{\vec{n}}_l$ denotes the unit vector in trend direction of the line, η is the trend of the line, and ε is the plunge.

B.2. Conversion from Cartesian coordinates to geological attitudes

In order to convert the Cartesian vector components $\begin{pmatrix} n_x \\ n_y \\ n_z \end{pmatrix}$ of a unit vector $\widehat{\vec{n}}$ (e.g. $\widehat{\vec{n}}_p$ or $\widehat{\vec{n}}_l$) into geological attitudes, several rules must be observed. The conversion to polar coordinates results in the trend and plunge of the line that contains $\widehat{\vec{n}}$.

From trigonometrical and geometrical relationships, the preliminary trend μ of the line can generally be calculated as

$$\mu = \arctan\left(\frac{n_y}{n_x}\right). \tag{B.2-1}$$

If $n_x = 0$, then the trend is calculated as

$$\mu = \frac{n_y}{|n_y|} \cdot 90°, \tag{B.2-2}$$

which means that the line would trend East–West. The first factor on the right hand side of Eq. (B.2-2) is normalised to ± 1.

If $n_x < 0$, then the calculation of the trend is

$$\mu = \arctan\left(\frac{n_y}{n_x}\right) + 180°, \tag{B.2-3}$$

meaning that $90° < \mu < 270°$. As in this case arctan results in negative (anti-clockwise) angles between the y-axis and the trendline, 180° have to be added to achieve a trend measured clockwise from North (x-axis).

If $\arctan((n_y)/(n_x)) < 0$, then the equation to determine the trend becomes

$$\mu = \arctan\left(\frac{n_y}{n_x}\right) + 360°. \tag{B.2-4}$$

In this case, the trend would be negative (anti-clockwise) from North (x-axis), thus 360° need to be added in order to achieve the correct trend measured clockwise from North.

The plunge ρ of the line is determined by

$$\rho = \arctan\left(\frac{n_z}{\sqrt{n_x^2 + n_y^2}}\right). \tag{B.2-5}$$

The only rule that applies for finding the plunge is that if $\sqrt{n_x^2 + n_y^2} = 0$, then the plunge is to be calculated as

$$\rho = \frac{n_z}{|n_z|} \cdot 90°. \tag{B.2-6}$$

This means that the line would be vertical.

Finally, in case the plunge is negative ($\rho < 0$), more rules apply for finding the correct trend μ_0 and plunge ρ_0.

If $\rho < 0$ and if $(\mu + 180°) > 360°$, then

$$\mu_0 = \mu - 180°. \tag{B.2-7}$$

If $\rho < 0$ and if $(\mu + 180°) < 360°$, then

$$\mu_0 = \mu + 180°. \tag{B.2-8}$$

In all other cases the true trend and plunge of the line are

$$\mu_0 = \mu \text{ and } \rho_0 = |\rho|. \tag{B.2-9}$$

Assuming $\widehat{\vec{n}}_p$ was the unit normal vector to a plane, and having derived the trend and plunge of the line that contains $\widehat{\vec{n}}_p$, the strike angle ξ and dip angle χ of the plane can be calculated observing the following rules:

If $90° + \mu_0 > 360°$, then the strike of the plane is given by

$$\xi = \mu_0 - 270°. \tag{B.2-10}$$

In all other cases, the strike is

$$\xi = \mu_0 + 90°, \tag{B.2-11}$$

and the dip of the plane is

$$\chi = 90° - \rho_0. \tag{B.2-12}$$

References

Cooper, M.A., Bamford, M.L.F., 1987. A note on photography in structural geology. Journal of Structural Geology 9, 121–126.

Fusseis, F., Handy, M.R., Schrank, C., 2006. Networking of shear zones at the brittle-to-viscous transition (Cap de Creus, NE Spain). Journal of Structural Geology 28, 1228–1234.

Pennacchioni, G., 2005. Control of the geometry of precursor brittle structures on the type of ductile shear zones in the Adamello tonalites, Southern Alps (Italy). Journal of Structural Geology 27, 627–644.

Ramsay, J.G., Huber, M.I., 1987. The Techniques of Modern Structural Geology, Vol. 2. Folds and Fractures. Academic Press, San Diego.

Talbot, C.J., 1999. Ductile shear zones as counterflow boundaries in pseudoplastic fluids. Journal of Structural Geology 21, 1535–1551.

Wightman, R.H., Prior, D.J., Little, T.A., 2006. Quartz veins deformed by diffusion creep-accommodated grain boundary sliding during a transient, high strain-rate event in the Southern Alps, New Zealand. Journal of Structural Geology 28, 902–918.